Supplement of Atmos. Chem. Phys., 26, 4313–4339, 2026
https://doi.org/10.5194/acp-26-4313-2026-supplement

Atmospheric Chemistry and Physics Open Access

Supplement of

Exceptional wildfire smoke over Greece in summer 2023: a synergistic study of aerosol optical-microphysical and UVB radiative impacts

Marilena Gidarakou et al.

Correspondence to: Marilena Gidarakou (marilenagidarakou@mail.ntua.gr) and Alexandros Papayannis (alexandros.papagiannis@epfl.ch)

Supplementary Material

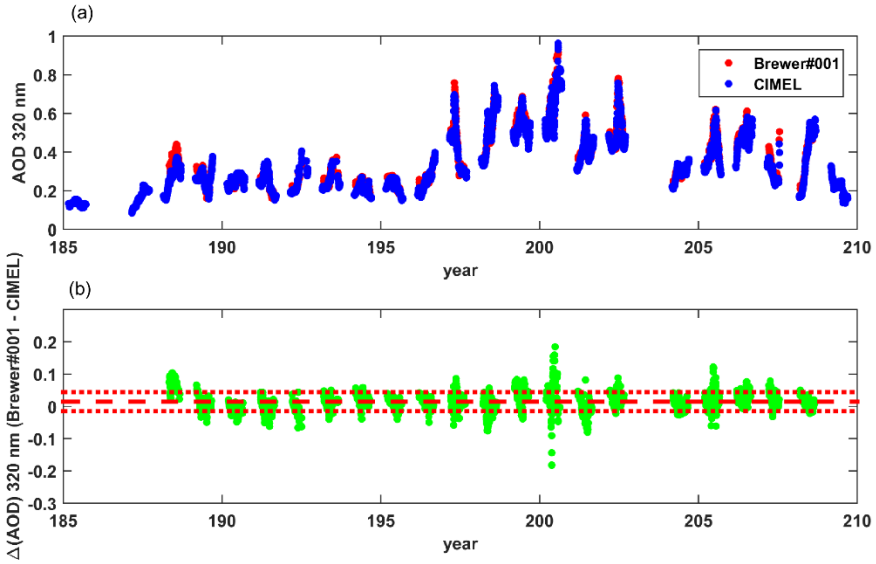

Figure S1. (a) Time series of AOD from Brewer (red) and CIMEL (blue) for the period 2023–2025. (b) Difference Δ(AOD) between Brewer and CIMEL AOD, for July - August 2023.

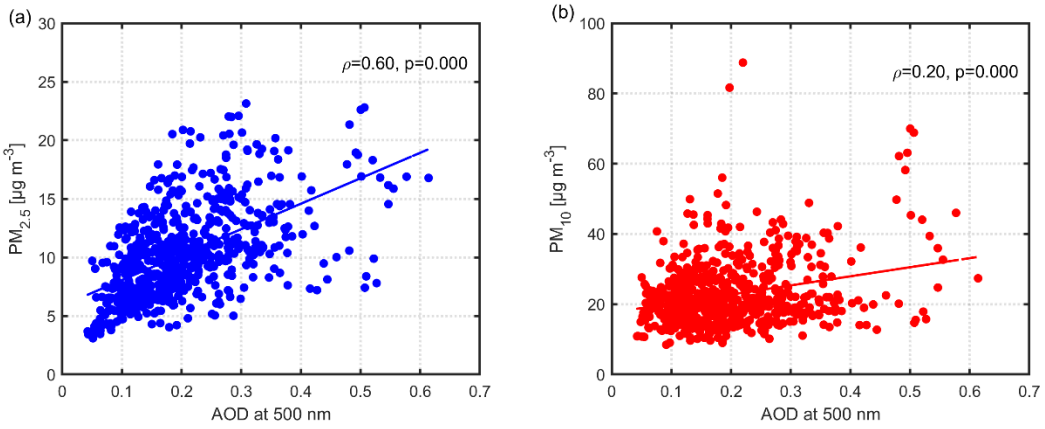

Figure S2. Spearman correlation between hourly (a) $PM_{2.5}$ and (b) PM_{10} concentrations and AOD at 500 nm during July and August 2023.

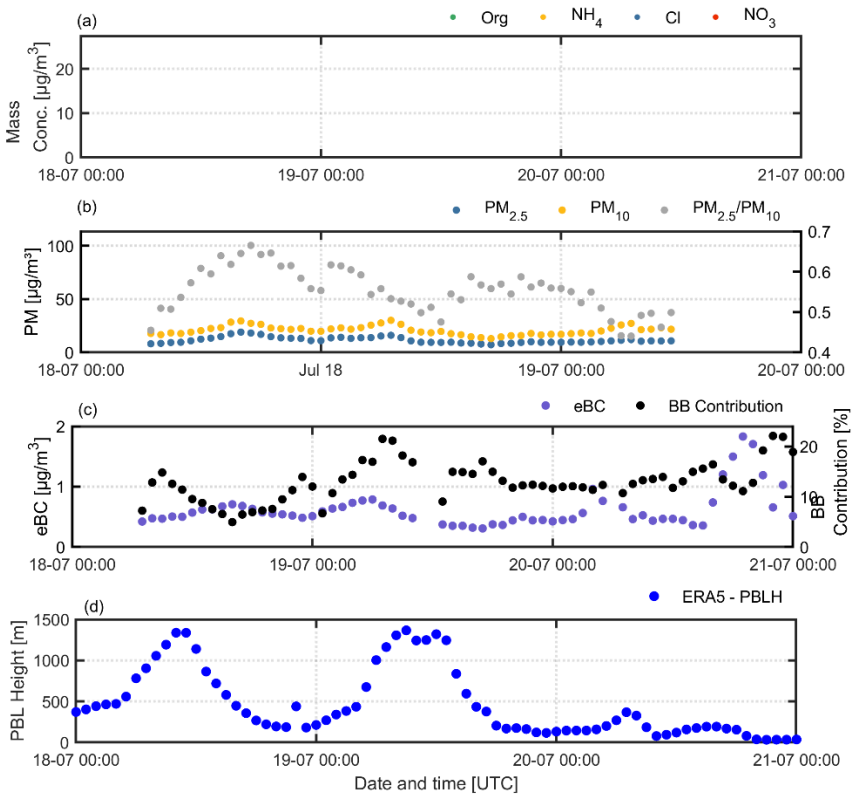

Figure S3. Time series of in-situ and reanalysis parameters illustrating the relationship between surface aerosol properties and boundary-layer evolution during the period of 18 – 21 July 2023. (a) Time−series of hourly averaged values of (a) AOD for various wavelengths (340 - 1020 nm) and AE at 440/870 nm obtained by the CIMEL sun-sky-lunar photometer and AOD at 320 nm obtained by the Brewer spectrophotometer (b) AOD and AE at 500 nm along with the Fine Mode Fraction (FMF) obtained by the CIMEL sun-sky-lunar photometer (c) mass concentration of various chemical composition (Org, NH_4^+, Cl, NO_3^-) obtained by ToF - ACSM (d) 1-h PM2.5 and PM10 concentration (e) eBC concentration and BB contribution obtained by the aethalometer. (d) ERA5 planetary boundary layer height (PBLH).

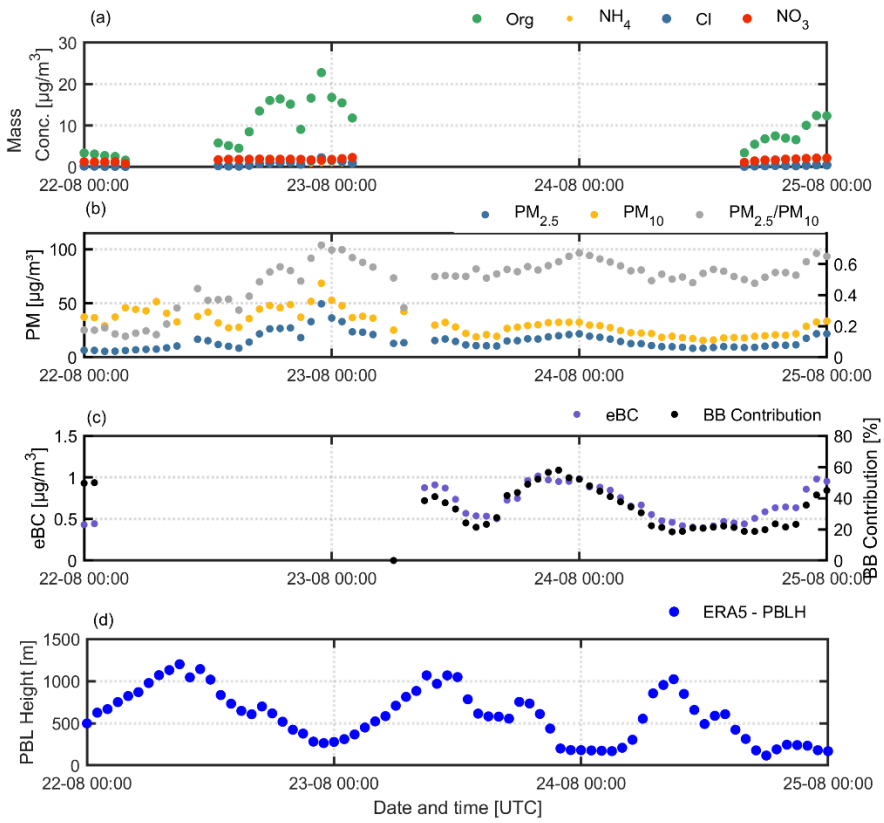

Figure S4. Time series of in-situ and reanalysis parameters illustrating the relationship between surface aerosol properties and boundary-layer evolution during the period of 22 – 25 August 2023. (a) Time–series of hourly averaged values of (a) AOD for various wavelengths (340 - 1020 nm) and AE at 440/870 nm obtained by the CIMEL sun-sky-lunar photometer and AOD at 320 nm obtained by the Brewer spectrophotometer (b) AOD and AE at 500 nm along with the Fine Mode Fraction (FMF) obtained by the CIMEL sun-sky-lunar photometer (c) mass concentration of various chemical composition (Org, NH_4^+, Cl, NO_3^-) obtained by ToF - ACSM (d) 1-h PM2.5 and PM10 concentration (e) eBC concentration and BB contribution obtained by the aethalometer. (d) ERA5 planetary boundary layer height (PBLH).

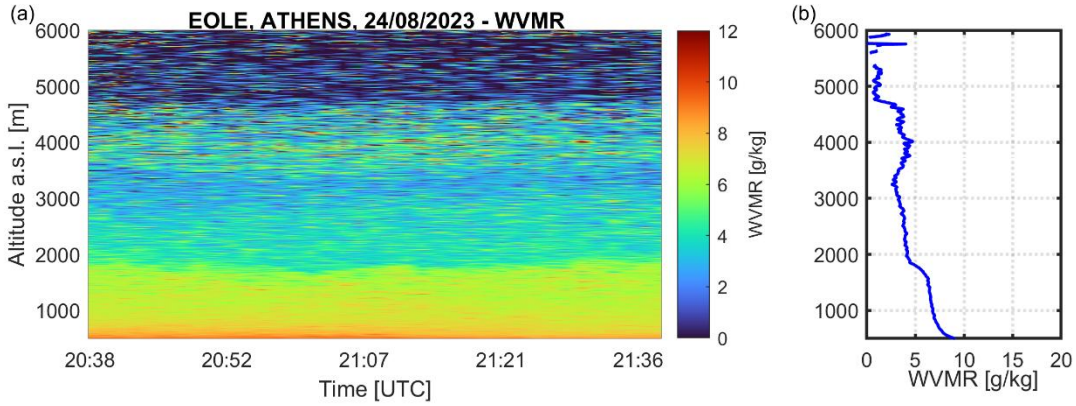

Figure S5. (a) Spatio-temporal evolution of the Water Vapor Mixing Ratio (WVMR) and (b) vertical profile of the WVMR obtained by EOLE lidar on 24 August 2023.

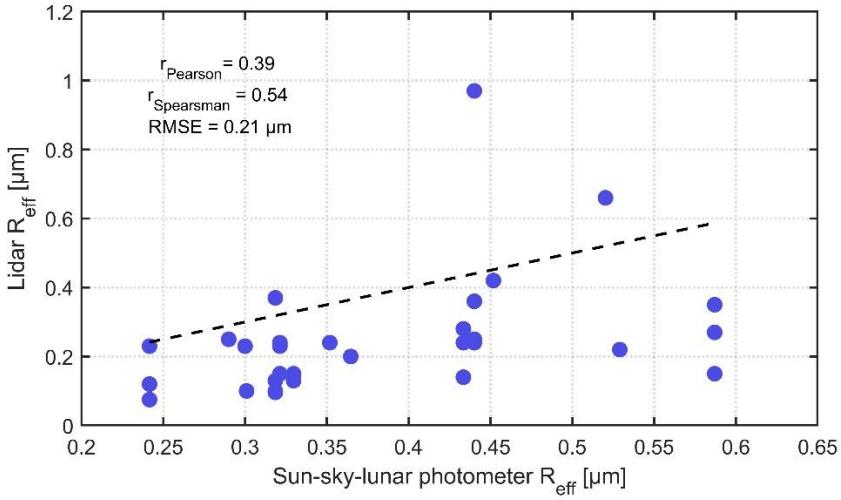

Figure S6. Comparison of lidar-retrieved and sun-sky-lunar photometer-retrieved R_{eff} for the period 17 July to 30 August 2023. The scatter plot shows individual observations, with the 1:1 line (dashed) indicating perfect agreement. Pearson and Spearman correlation coefficients, root-mean-square error (RMSE), and mean bias (Lidar − Sun) are reported in the panel.

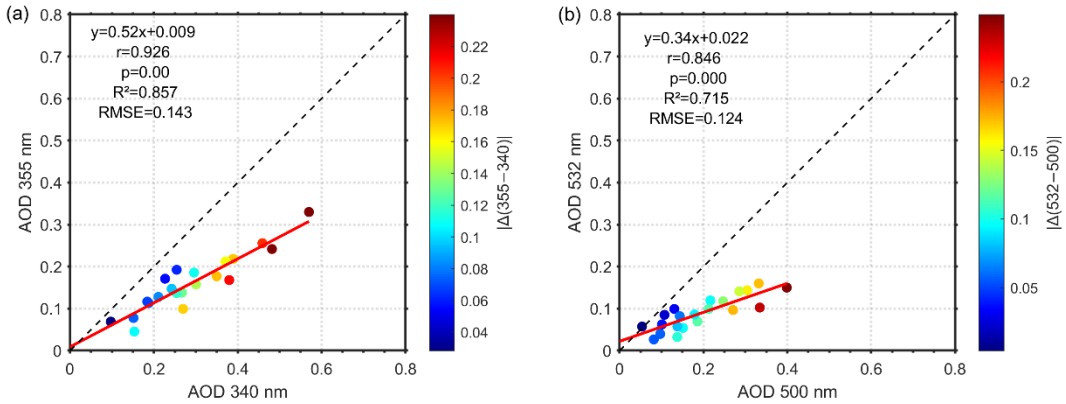

Figure S7. Comparison of layer-integrated AOD retrieved from the lidar with CIMEL sun-photometer measurements. (a) 355 nm (Lidar) vs. 340 nm (CIMEL) and (b) 532 nm (Lidar) vs. 500 nm (CIMEL).

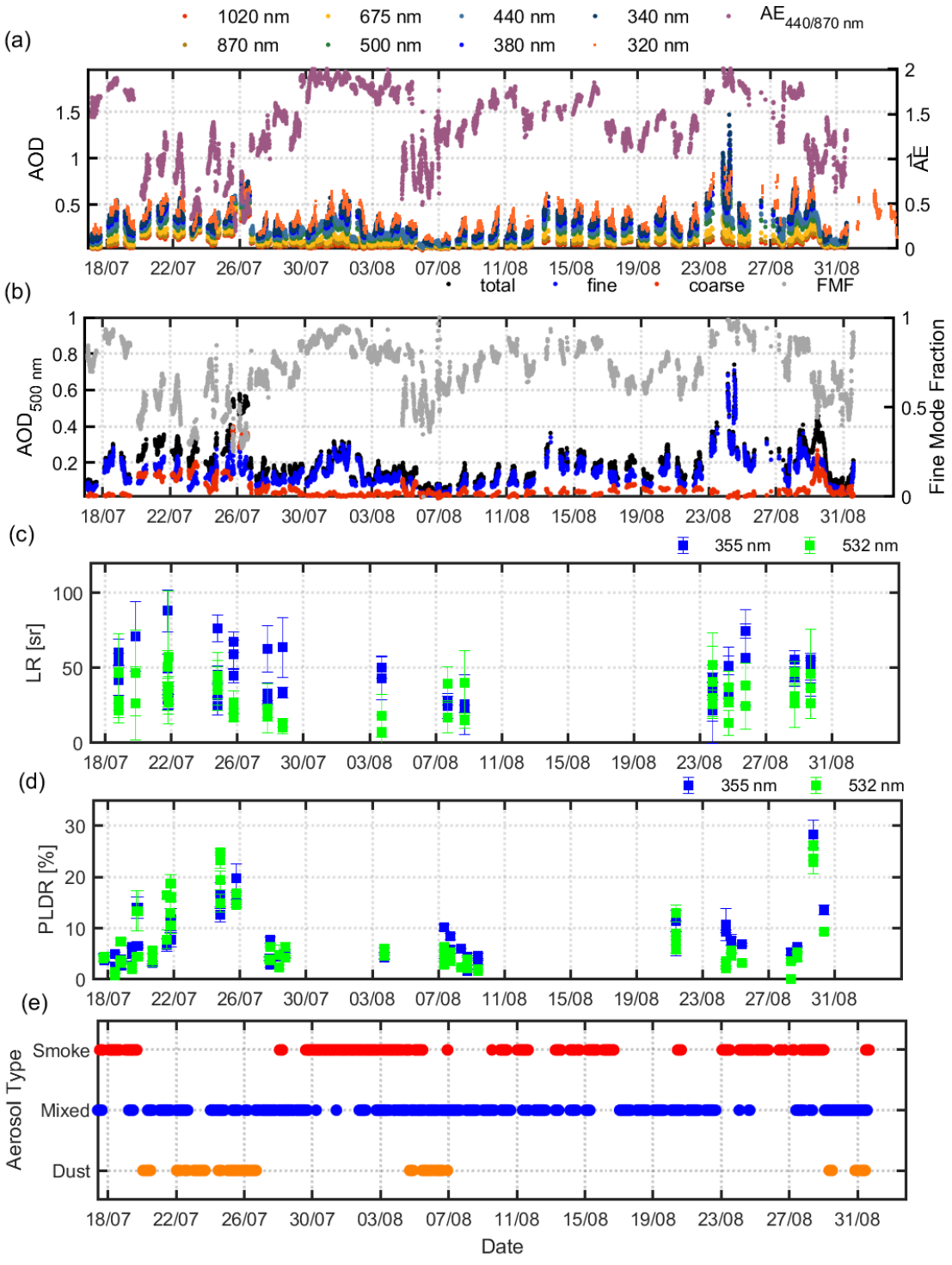

Figure S8. Time−series of hourly averaged values of (a) AOD for various wavelengths (340 - 1020 nm) and AE at 440/870 nm obtained by the CIMEL sun-sky-lunar photometer (b) AOD and AE at 500 nm along with the Fine Mode Fraction (FMF) obtained by the CIMEL sun-sky-lunar photometer (c) LR at 355 and 532 nm, (d) lidar particle depolarization ratio at 532, (e) Multi-platform aerosol classification.